$O(1/M^3)$ effects for heavy-light mesons in lattice NRQCD

Randy Lewis
Jefferson Lab, 12000 Jefferson Avenue, Newport News, Virginia 23606
and Department of Physics, University of Regina, Regina, Saskatchewan, Canada S4S 0A2

R. M. Woloshyn
TRIUMF, 4004 Wesbrook Mall, Vancouver, British Columbia, Canada V6T 2A3

(Received 4 March 1998; revised manuscript received 1 June 1998; published 2 September 1998)

The masses of $^1S_0$ and $^3S_1$ mesons containing a single heavy quark are computed in the quenched approximation. The light quark action and gauge field action are both classically improved and tadpole improved, and the couplings to the heavy quark are organized by the $1/M$ expansion of tadpole-improved NRQCD. At each of two lattice spacings, near 0.22 fm and 0.26 fm, meson masses are obtained for heavy quarks spanning the region between charmed and bottom mesons. Results up to $O(1/M)$, $O(1/M^2)$ and $O(1/M^3)$ are displayed separately, so that the convergence of the heavy quark expansion can be discussed. Also, the effect of each term in the $O(1/M^3)$ contribution is computed individually. For bottom mesons the $1/M$ expansion appears to be satisfactory, but the situation for charmed mesons is less clear. [S0556-2821(98)03619-4]

PACS number(s): 12.38.Gc, 14.40.Lb, 14.65.Dw, 14.65.Fy

I. INTRODUCTION

Long-distance, nonperturbative QCD interactions can be studied numerically by discretizing space-time, if the lattice spacing ''a'' is sufficiently small to allow a matching to perturbative QCD. To include the effects of a quark whose inverse mass is smaller than the lattice spacing, it is natural to use an effective Lagrangian which is ordered by powers of the inverse quark mass. Two different notations which have been used for this expansion are heavy quark effective theory (HQET) [1] and nonrelativistic QCD (NRQCD) [2,3].

In the present work, the NRQCD formalism is used to study the masses of the ground state ($^1S_0$) and first excited state ($^3S_1$) heavy-light mesons, i.e. mesons containing a single heavy quark. These masses are well-known experimentally [4], and have been previously determined from lattice NRQCD [5–9] up to $O(1/M^2)$. The primary goal of the present research is to extend the calculation to $O(1/M^3)$, and to display the effects of each new term individually. This provides an indication of the convergence of the $1/M$ expansion of lattice NRQCD. Of particular interest are the physically relevant cases of charmed and bottom mesons, both of which will be discussed herein.

To allow the use of coarsely spaced lattices, the light-quark and gauge terms in the action will be classically improved, and the entire action will be tadpole improved. Not only does a larger lattice spacing imply speedier simulations, but it also means that the minimum heavy quark mass of NRQCD (which is of the order of the inverse lattice spacing) is reduced. This opens the possibility of using NRQCD to study charmed mesons.

Lattice NRQCD has been used extensively for studies of quarkonium [10], where the $1/M$ expansion is replaced by a velocity expansion, and it was concluded that the velocity expansion for the spin splitting of charmonium S waves does not converge very quickly [11]. In the present work, the spin splittings of S-wave heavy-light charmed mesons nicely satisfy $|O(1/M^3)|<|O(1/M^2)|<|O(1/M)|$. However, there is an individual $O(1/M^3)$ term which is larger in magnitude than the total $O(1/M^2)$ contribution. Future studies may be able to improve this situation, and various suggestions present themselves as conclusions to this exploratory study.

II. ACTION

The lattice action can be written as the sum of three terms:

$$S=S_G(U)+S_q(\overline{q},q;U)+S_Q(\overline{Q},Q;U), \tag{1}$$

where U, q and Q are the gauge field, light quark field and heavy quark field, respectively.

Following the work of Lüscher and Weisz [12], a gauge field action which is classically correct up to $O(a^4)$ errors can be written by including a sum over 1×2 rectangular plaquettes (U_{rt}) as well as 1×1 elementary plaquettes (U_{pl}):

$$S_G(U)=\frac{\beta}{3}\mathrm{ReTr}\left[\sum_{pl}(1-U_{pl})-\frac{1}{20U_0^2}\sum_{rt}(1-U_{rt})\right]. \tag{2}$$

A tadpole factor, defined by

$$U_0=\left\langle\frac{1}{3}\mathrm{ReTr}U_{pl}\right\rangle^{1/4} \tag{3}$$

has been introduced to absorb the lattice tadpole effects and thereby improve the matching to perturbation theory [13].

A light quark action, with classical errors at $O(a^2)$ in spectral quantities, has been constructed by Sheikholeslami and Wohlert [14]:

$$S_q(\overline{q},q;U)=-\sum_x \overline{q}(x)q(x)$$
$$+\kappa\sum_{x,\mu}[\overline{q}(x)(1-\gamma_\mu)U_\mu(x)q(x+\mu)$$
$$+\overline{q}(x+\mu)(1+\gamma_\mu)U_\mu^\dagger(x)q(x)]$$
$$-\frac{g\kappa}{2U_0^3}\sum_{x,\mu,\nu}\overline{q}(x)\sigma_{\mu\nu}F_{\mu\nu}(x)q(x). \quad (4)$$

Again, the tadpole factor has been included for the reduction of quantum discretization errors. The lattice field strength tensor is given by

$$gF_{\mu\nu}(x)=\frac{1}{2i}(\Omega_{\mu\nu}(x)-\Omega_{\mu\nu}^\dagger(x))-\frac{1}{3}\mathrm{Im}(\mathrm{Tr}\Omega_{\mu\nu}(x)), \quad (5)$$

$$\Omega_{\mu\nu}=\frac{-1}{4}[U_\mu(x)U_\nu(x+\hat{\mu})U_\mu^\dagger(x+\hat{\nu})U_\nu^\dagger(x)$$
$$+U_\nu(x)U_\mu^\dagger(x-\hat{\mu}+\hat{\nu})U_\nu^\dagger(x-\hat{\mu})U_\mu(x-\hat{\mu})$$
$$+U_\mu^\dagger(x-\hat{\mu})U_\nu^\dagger(x-\hat{\mu}-\hat{\nu})U_\mu(x-\hat{\mu}-\hat{\nu})U_\nu(x-\hat{\nu})$$
$$+U_\nu^\dagger(x-\hat{\nu})U_\mu(x-\hat{\nu})U_\nu(x+\hat{\mu}-\hat{\nu})U_\mu^\dagger(x)]. \quad (6)$$

For quarkonium, the form of the heavy quark action has been discussed in detail by Lepage *et al.* [3]. It is convenient to write the heavy quark action in terms of the Hamiltonian H:

$$S_Q(\overline{Q},Q;U)=\int \mathrm{d}^4x\ Q^\dagger(x)(iD_t-H)Q(x). \quad (7)$$

To discuss heavy-light mesons, it is appropriate to reorganize the velocity expansion of H, discussed in Ref. [3], into an expansion in powers of the inverse heavy quark bare mass M:

$$H=H_0+\delta H^{(1)}+\delta H^{(2)}+\delta H^{(3)}+O(1/M^4) \quad (8)$$

$$H_0=\frac{-\Delta^{(2)}}{2M} \quad (9)$$

$$\delta H^{(1)}=-\frac{c_4}{U_0^4}\frac{g}{2M}\boldsymbol{\sigma}\cdot\tilde{\mathbf{B}}+c_5\frac{a^2\Delta^{(4)}}{24M}, \quad (10)$$

$$\delta H^{(2)}=\frac{c_2}{U_0^4}\frac{ig}{8M^2}(\tilde{\boldsymbol{\Delta}}\cdot\tilde{\mathbf{E}}-\tilde{\mathbf{E}}\cdot\tilde{\boldsymbol{\Delta}})$$
$$-\frac{c_3}{U_0^4}\frac{g}{8M^2}\boldsymbol{\sigma}\cdot(\tilde{\boldsymbol{\Delta}}\times\tilde{\mathbf{E}}-\tilde{\mathbf{E}}\times\tilde{\boldsymbol{\Delta}})-c_6\frac{a(\Delta^{(2)})^2}{16nM^2}, \quad (11)$$

$$\delta H^{(3)}=-c_1\frac{(\Delta^{(2)})^2}{8M^3}-\frac{c_7}{U_0^4}\frac{g}{8M^3}\{\tilde{\Delta}^{(2)},\boldsymbol{\sigma}\cdot\tilde{\mathbf{B}}\}$$
$$-\frac{c_9}{U_0^8}\frac{ig^2}{8M^3}\boldsymbol{\sigma}\cdot(\tilde{\mathbf{E}}\times\tilde{\mathbf{E}}+\tilde{\mathbf{B}}\times\tilde{\mathbf{B}})$$
$$-\frac{c_{10}}{U_0^8}\frac{g^2}{8M^3}(\tilde{\mathbf{E}}^2+\tilde{\mathbf{B}}^2)-c_{11}\frac{a^2(\Delta^{(2)})^3}{192n^2M^3}. \quad (12)$$

The coefficients of the Hamiltonian are chosen so the dimensionless parameters, c_i, are unity at the classical level. Terms arising from quantum effects, i.e. containing powers of g unaccompanied by **E** or **B**, have not been shown. A tilde on any quantity indicates that the leading discretization errors have been removed. In particular,

$$\tilde{E}_i=\tilde{F}_{4i}, \quad (13)$$

$$\tilde{B}_i=\frac{1}{2}\epsilon_{ijk}\tilde{F}_{jk} \quad (14)$$

where [3]

$$\tilde{F}_{\mu\nu}(x)=\frac{5}{3}F_{\mu\nu}(x)-\frac{1}{6U_0^2}[U_\mu(x)F_{\mu\nu}(x+\hat{\mu})U_\mu^\dagger(x)$$
$$+U_\mu^\dagger(x-\hat{\mu})F_{\mu\nu}(x-\hat{\mu})U_\mu(x-\hat{\mu})$$
$$-(\mu\leftrightarrow\nu)]. \quad (15)$$

The various lattice derivatives are defined as follows:

$$a\Delta_iG(x)=\frac{1}{2U_0}[U_i(x)G(x+a\hat{\imath})$$
$$-U_i^\dagger(x-a\hat{\imath})G(x-a\hat{\imath})] \quad (16)$$

$$a\Delta_i^{(+)}G(x)=\frac{U_i(x)}{U_0}G(x+a\hat{\imath})-G(x) \quad (17)$$

$$a\Delta_i^{(-)}G(x)=G(x)-\frac{U_i^\dagger(x-a\hat{\imath})}{U_0}G(x-a\hat{\imath}) \quad (18)$$

$$a^2\Delta_i^{(2)}G(x)=\frac{U_i(x)}{U_0}G(x+a\hat{\imath})-2G(x)$$
$$+\frac{U_i^\dagger(x-a\hat{\imath})}{U_0}G(x-a\hat{\imath}) \quad (19)$$

$$\tilde{\Delta}_i=\Delta_i-\frac{a^2}{6}\Delta_i^{(+)}\Delta_i\Delta_i^{(-)} \quad (20)$$

$$\Delta^{(2)}=\sum_i \Delta_i^{(2)} \quad (21)$$

$$\tilde{\Delta}^{(2)}=\Delta^{(2)}-\frac{a^2}{12}\Delta^{(4)} \tag{22}$$

$$\Delta^{(4)}=\sum_i\ (\Delta_i^{(2)})^2. \tag{23}$$

All of the terms in Eqs. (9)–(12) appear in Ref. [3] except for the pieces of the c_9 and c_{10} terms quadratic in $\tilde{\mathbf{B}}$ (because they are of negligibly high order for quarkonium) and the c_{11} term (to be discussed below). The fact that the Hamiltonian H is complete to $O(1/M^3)$ in the classical continuum limit has been shown by Manohar [15].

It is conventional to separate H into two pieces, H_0 and δH, such that the evolution of a heavy quark Green's function takes the form [3,16]

$$G_1=\left(1-\frac{aH_0}{2n}\right)^n\frac{U_4^\dagger}{U_0}\left(1-\frac{aH_0}{2n}\right)^n\ \delta_{\vec{x},0} \tag{24}$$

$$G_{t+1}=\left(1-\frac{aH_0}{2n}\right)^n\frac{U_4^\dagger}{U_0}\left(1-\frac{aH_0}{2n}\right)^n \times(1-a\,\delta H)G_t,\quad t>0 \tag{25}$$

where n is a parameter which should be chosen to stabilize the numerics. Notice that for a free heavy quark field, the only relevant terms in the Hamiltonian are H_0 and the terms containing c_1, c_5, c_6 or c_{11}. Setting each of these c_i to its classical value of unity, and working consistently to $O(1/M^3)$, gives

$$G_{t+1}=\exp\left[-a\left(H_0-\frac{(\Delta^{(2)})^2}{8M^3}+O(a^3)\right)\right]G_t,\quad \text{for } t>0 \tag{26}$$

which displays the absence of discretization errors for the free quark Hamiltonian up to $O(a^2)$. The terms containing explicit powers of ''a'' (c_5, c_6 and c_{11}) were added to the Hamiltonian precisely for this purpose.

III. CORRELATION FUNCTIONS

A heavy-light meson is created by the following operator:

$$\sum_{\vec{x}}\ Q^\dagger(\vec{x})\Gamma(\vec{x})q(\vec{x}), \tag{27}$$

where $\Gamma(\vec{x})$ is a 4×2 matrix containing the spin structure

$$^1S_0:\Gamma(\vec{x})=\begin{pmatrix}0 & I\end{pmatrix}, \tag{28}$$

$$^3S_1:\Gamma(\vec{x})=\begin{pmatrix}0 & \sigma_i\end{pmatrix}. \tag{29}$$

Gauge-invariant smearing was also tried according to the method described in Ref. [11], but it provided no significant improvement for the heavy-light S waves, which already display clear plateaus for local sources and sinks.

The general form of the meson correlation function is

$$G_{\rm meson}(\vec{p},t)=\sum_{\vec{y}}\ \mathrm{Tr}[\,\gamma_5(M^{-1})^\dagger(\vec{y}-\vec{x})\,\gamma_5 \times\Gamma_{(sk)}^\dagger(\vec{y})G_t(\vec{y}-\vec{x})\Gamma_{(sc)}(\vec{x})] \times\exp(-i\vec{p}\cdot(\vec{y}-\vec{x})). \tag{30}$$

Because NRQCD is an expansion in the inverse *bare* heavy quark mass, all meson mass differences can be obtained from correlation functions at $\vec{p}=\vec{0}$, but the absolute meson mass itself remains undetermined. One way to fix the mass is to compute the change in energy when a meson is boosted:

$$E_{\mathbf{p}}-E_0=\frac{\mathbf{p^2}}{2M_{\rm kin}}. \tag{31}$$

This defines the kinetic mass, $M_{\rm kin}$, which is interpreted as the meson's physical mass. For the present work, $E_{\mathbf{p}}$ is computed only for the $^1S_0$ state, with $\mathbf{p}=(0,0,2\pi/L_s)$ where L_s is the spatial extent of the lattice.

IV. RESULTS

Gauge field configurations, periodic at all lattice boundaries, were generated using a pseudo-heatbath algorithm. After 4000 thermalizing sweeps, the retained configurations were separated from one another by 250 sweeps. Light quark matrix inversion was performed by a stabilized biconjugate gradient algorithm, also periodic at the lattice boundaries.

Although the light quark field is periodic in each space-time direction, Eqs. (24),(25) indicate that the heavy quark field is periodic only in the spatial directions. Therefore, the correlation functions for heavy-light mesons are only useful for times smaller than about $L_t/2$, where L_t is the temporal extent of the lattice. Figure 1 shows examples of effective mass plots for $^1S_0$ and $^3S_1$ charmed mesons, where

$$m_{\rm eff}(\tau)=-\ln\left(\frac{G_{\rm meson}(\vec{p},\tau+1)}{G_{\rm meson}(\vec{p},\tau)}\right). \tag{32}$$

In all cases, a plateau is found where the effective mass values computed at three (or more) neighboring timeslices are equal within the bootstrap errors.

The mass of a $^1S_0$ heavy-light meson is taken to be the average of all effective mass values within the plateau region. The uncertainty associated with this mass is determined by a bootstrap procedure, where 1000 bootstrap ensembles are chosen from the original data such that each ensemble is the same size as the original data sample. A bootstrap distribution is then obtained by computing, for each ensemble, the average of all effective mass values within the plateau region. The uncertainty in the meson mass is then taken to be half the distance between the 16th and 84th percentiles in the bootstrap distribution.

The same method could be applied to the mass of the $^3S_1$, but the errors are expected to be highly correlated with those in the $^1S_0$ calculation. Therefore, the $^3S_1-{}^1S_0$ mass difference is determined by applying the bootstrap technique directly to the mass difference.

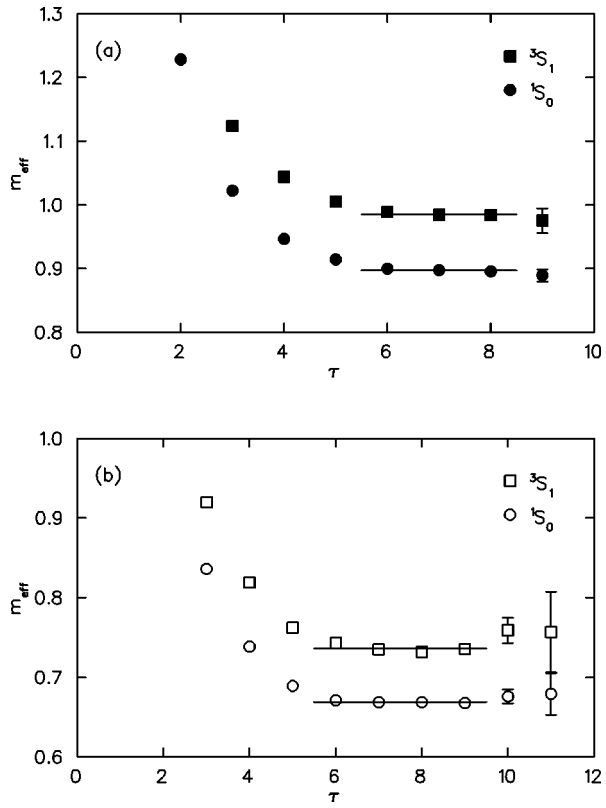

FIG. 1. Effective mass plots for $^1S_0$ and $^3S_1$ charmed mesons at rest, including terms up to $O(1/M^3)$. Solid symbols denote data at $\beta=6.8$, $aM=1.43$ and $\kappa=0.135$, while open symbols correspond to $\beta=7.0$, $aM=1.10$ and $\kappa=0.134$. The meson source is at $\tau=1$. Horizontal lines indicate masses extracted from the plateau regions.

Some parameters of the simulations are given in Table I. The determinations of κ_c, κ_s and a_ρ come from separate simulations involving 250 configurations at $\beta=6.8$ and 200 configurations at $\beta=7.0$. The values of U_0 agree with Ref. [11]. The stabilizing parameter n of Eqs. (24),(25) was at least as large as $n=4$ for $aM<1.2$, $n=3$ for $1.2\leqslant aM<1.5$ and $n=2$ for $aM\geqslant 1.5$ [11].

The bare charm quark masses at $\beta=6.8$ and $\beta=7.0$ were obtained in Ref. [11] by equating the kinetic mass of the η_c with its physical mass. This calculation can be reproduced (with poorer statistics) using the gauge field configurations of Table I, provided that one additional term is added to the Hamiltonian of Eqs. (8)–(12):

$$H_{full}=H-\frac{c_8}{U_0^4}\frac{3g}{64M^4}\{\tilde{\Delta}^{(2)},\boldsymbol{\sigma}\cdot(\tilde{\boldsymbol{\Delta}}\times\tilde{\mathbf{E}}-\tilde{\mathbf{E}}\times\tilde{\boldsymbol{\Delta}})\}. \quad (33)$$

For heavy-light calculations the term containing c_8 is suppressed by four powers of $1/M$, but in the velocity expansion relevant to quarkonium it contributes at $O(v^6)$, and is the only $O(v^6)$ term absent in Eqs. (8)–(12). As was done in all other terms, the parameter c_8 is here set to its classical value of unity.

It is also worth noting that H_{full} contains terms which are beyond $O(v^6)$ in the velocity expansion. The minimal Hamiltonian up to $O(v^6)$ is obtained from H_{full} by omitting the portions of the c_9 and c_{10} terms which involve two powers of $\tilde{\mathbf{B}}$. It is typical to neglect the c_{11} term as well. In Ref. [11], the entire c_{10} term was also omitted, since it contains no spin structure and therefore seemed negligible for a discussion of quarkonium spin splittings. (This point will be addressed below in the context of heavy-light mesons.) The resulting Hamiltonian will be referred to as H_{spin}.

Table II shows a good agreement between the bare charm quark masses obtained here and those of Ref. [11]. The bare bottom quark mass can be obtained in a similar fashion, using the η_b in place of the η_c. Because the η_b has not yet been seen experimentally, its ''physical mass'' is obtained by subtracting the hyperfine splitting (of the present lattice simulations) from the experimental Υ mass. In practice, the hyperfine splitting is a negligible subtraction in comparison with the simulation uncertainties. The resulting values for M_b are shown in Table II.

Table II indicates that for $M\approx M_b$, the terms which distinguish between H_{spin} and H_{full} are negligibly small in comparison with the computational uncertainties. Some evidence of their effect might be seen near $M=M_c$, but the large uncertainties do not allow a definitive statement to be made. A more precise comparison of H_{spin} and H_{full} can be obtained from the quarkonium spin splittings, but this is not required for the present study.

Having fixed all lattice parameters from light-light and heavy-heavy meson observables, the heavy-light spectrum will now be considered. Figure 2 shows the simulation energy of a $^1S_0$ heavy-light meson as a function of the bare heavy quark mass, computed to $O(1/M)$, $O(1/M^2)$ and $O(1/M^3)$. For each β, the light quark mass is fixed at a value slightly less than twice the strange quark mass, according to Table I. Figure 2 indicates that terms beyond $O(1/M)$ provide small corrections to the leading order result when $M\approx M_b$, but these corrections grow as M decreases. Near $M=M_c$, the effect of $O(1/M^3)$ terms is larger than the $O(1/M^2)$ terms.

In order to understand the origin of such large $O(1/M^3)$ contributions in the charm region, simulations were performed with each $O(1/M^3)$ term added individually to the

TABLE I. Simulation parameters. N_U is the number of gauge field configurations, κ_c is the hopping parameter at the critical point, κ_s is the hopping parameter corresponding to the strange quark mass (from $m_{K*}/m_K=1.8$) and a_ρ is the lattice spacing derived from the ρ meson mass.

Lattice	N_U	β	κ	U_0	κ_c	κ_s	a_ρ [fm]
$8^3\times 14$	400	6.8	0.135, 0.138, 0.141	0.854	0.1458(1)	0.1398(4)	0.260(6)
$10^3\times 16$	300	7.0	0.134, 0.137, 0.140	0.865	0.1434(1)	0.1385(3)	0.225(8)

TABLE II. Values for the lattice spacing as derived from the $1P$-$1S$ mass splitting of charmonium, and values for the heavy quark masses. Both masses from Ref. [11] lead to $M_{\eta_c}=2.9(1)$ GeV. All other entries show the range of aM_c and aM_b which reproduce the actual experimental values for M_{η_c} and M_Υ.

β	$a_{\rm hvy}$ [fm]	aM_c			aM_b	
	(Ref. [11])	H_{spin} (Ref. [11])	H_{spin}	H_{full}	H_{spin}	H_{full}
6.8	0.257(9)	1.43	1.5(1)	1.7(1)	5.0(2)	5.0(2)
7.0	0.205(9)	1.10	1.1(1)	1.1(1)	4.2(1)	4.2(1)

lower-order Hamiltonian. Results for the simulation energy are shown in Fig. 3. Apparently, all terms except the c_{10} term offer only modest corrections to the lower-order result. In fact, the c_{10} term is unique because it is the only term in the Hamiltonian [up to $O(1/M^3)$] which has a nonzero vacuum expectation value [17]. This vacuum value is simply an $O(1/M^3)$ shift of the bare heavy quark mass, and therefore produces an $O(1/M^3)$ shift in the meson simulation energy.

The vacuum expectation value can be computed directly from the gauge field configurations of Table I by averaging over all lattice sites:

$$a^4\left\langle \frac{g^2}{U_0^8}(\tilde{\mathbf{E}}^2+\tilde{\mathbf{B}}^2)\right\rangle=\begin{cases}13.6161(20) & \text{for } \beta=6.8,\\ 12.0716(16) & \text{for } \beta=7.0.\end{cases} \quad (34)$$

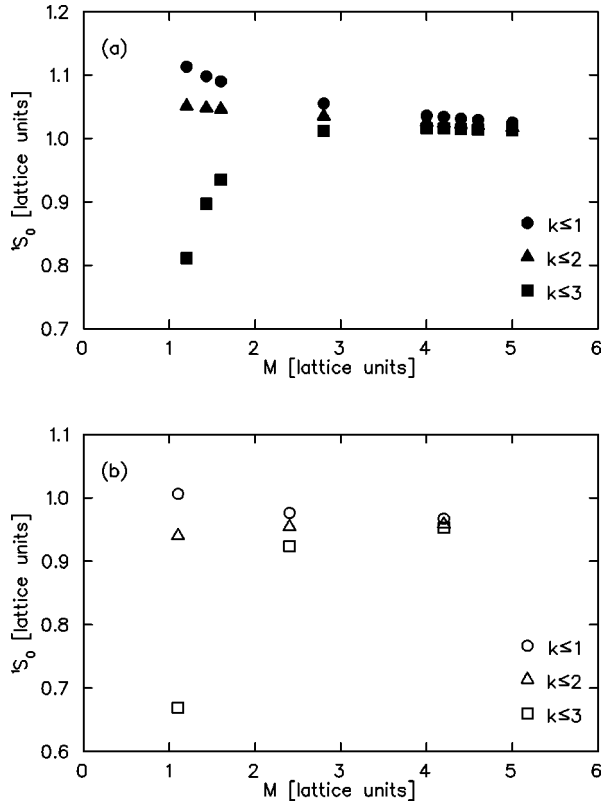

FIG. 2. The simulation energy of a ground state heavy-light meson at rest. Results are displayed from terms up to $O(1/M^k)$, with $k=1,2,3$. M is the bare heavy quark mass. Solid symbols denote data at $\beta=6.8$ and $\kappa=0.135$, while open symbols correspond to $\beta=7.0$ and $\kappa=0.134$.

If the vacuum expectation value is removed from the action,

$$\delta S_Q=\frac{c_{10}}{8M^3}\int \mathrm{d}^4x\ Q^{a\dagger}(x)\frac{g^2}{U_0^8}(\tilde{\mathbf{E}}^2+\tilde{\mathbf{B}}^2)^{ab}Q^b(x)$$
$$\to\frac{c_{10}}{8M^3}\int \mathrm{d}^4x\ Q^{a\dagger}(x)\left[\frac{g^2}{U_0^8}(\tilde{\mathbf{E}}^2+\tilde{\mathbf{B}}^2)^{ab}-\frac{\delta^{ab}}{3}\left\langle\frac{g^2}{U_0^8}(\tilde{\mathbf{E}}^2+\tilde{\mathbf{B}}^2)\right\rangle\right]Q^b(x), \quad (35)$$

then the contribution of the c_{10} term to the simulation energy is reduced to the size of the other $O(1/M^3)$ terms, as shown in Fig. 4. Removal of the vacuum expectation value from the action is justified because it is simply an addition to the heavy quark mass, which has already been removed from the Hamiltonian, Eq. (8), by the standard heavy-field transformation of HQET. Mass *differences* should not depend on whether or not the vacuum expectation value remains explicitly in the Hamiltonian.

Figure 5 displays the energy splitting between a $^1S_0$ meson at zero and nonzero 3-momenta. The vacuum expectation value has not been removed from the c_{10} term, but its effect should cancel in the difference between zero and nonzero 3-momenta. Figure 5 shows that the $O(1/M^2)$ and $O(1/M^3)$ terms offer only small corrections to the leading contribution, so a determination of the kinetic mass from Eq. (31) will not depend sensitively on the presence of these terms.

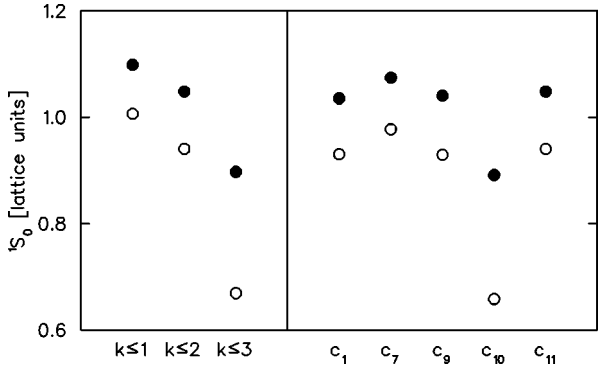

FIG. 3. The simulation energy of a ground state charmed meson at rest. Results are displayed from terms up to $O(1/M^k)$, with $k=1,2,3$. Solid symbols denote data at $\beta=6.8$, $\kappa=0.135$ and $aM=1.43$, while open symbols correspond to $\beta=7.0$, $\kappa=0.134$ and $aM=1.10$. To the right of the vertical line, the effect of adding each $O(1/M^3)$ term to the $O(1/M^2)$ Hamiltonian is shown individually.

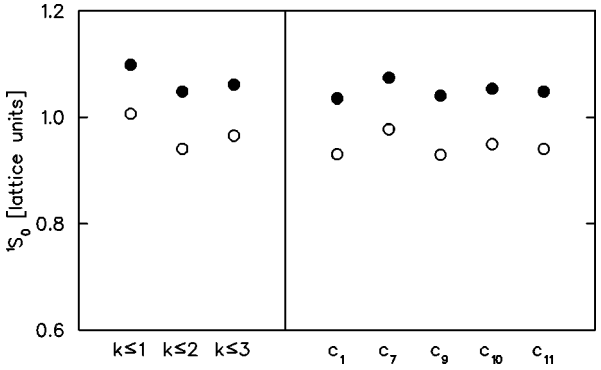

FIG. 4. These data are identical to Fig. 3 except that the vacuum expectation value has here been subtracted from the c_{10} term.

Figure 6 gives the contribution of each $O(1/M^3)$ term to the energy splitting between a $^1S_0$ meson at zero and nonzero 3-momenta. The contribution of each term is small in comparison to the statistical uncertainties, including the c_{10} term. (As expected, both Figs. 5 and 6 remain essentially unaltered if the vacuum expectation value is subtracted.)

Figure 5 raises another important issue. Because the bare quark mass is not a physical parameter, it is not necessarily sensible to compare the results of the $O(1/M)$, $O(1/M^2)$ and

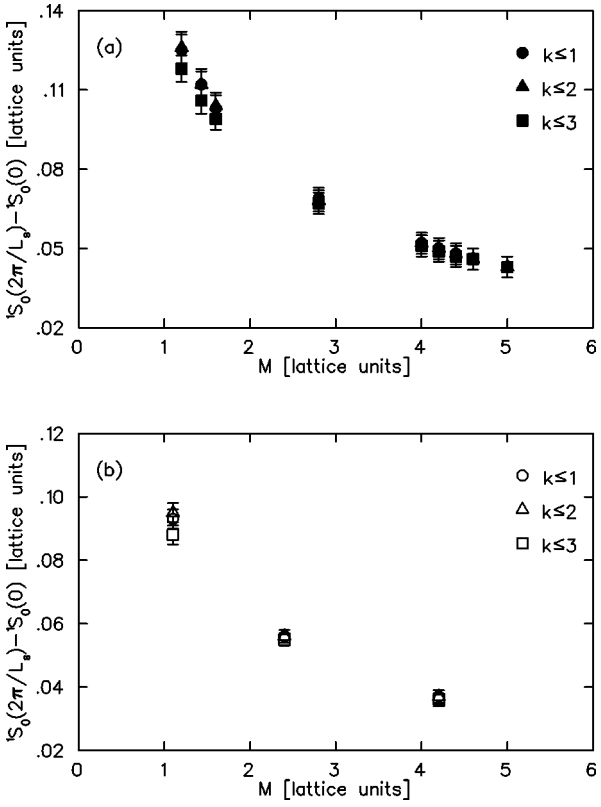

FIG. 5. The energy splitting between a ground state heavy-light meson with momentum $\vec{p}=(0,0,2\pi/L_s)$ (where L_s is the spatial extent of the lattice) and the same meson at rest. Results are displayed from terms up to $O(1/M^k)$, with $k=1,2,3$. M is the bare heavy quark mass. Solid symbols denote data at $\beta=6.8$ and $\kappa=0.135$, while open symbols correspond to $\beta=7.0$ and $\kappa=0.134$.

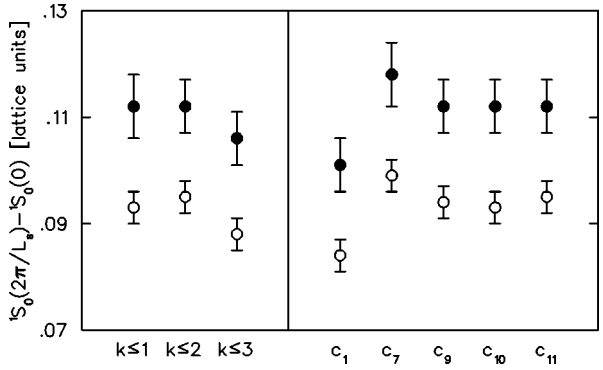

FIG. 6. The energy splitting between a ground state charmed meson with momentum $2\pi/L_s$ (where L_s is the spatial extent of the lattice) and the same meson at rest. Results are displayed from terms up to $O(1/M^k)$, with $k=1,2,3$. Solid symbols denote data at $\beta=6.8$, $\kappa=0.135$ and $aM=1.43$, while open symbols correspond to $\beta=7.0$, $\kappa=0.134$ and $aM=1.10$. To the right of the vertical line, the effect of adding each $O(1/M^3)$ term to the $O(1/M^2)$ Hamiltonian is shown individually.

$O(1/M^3)$ Hamiltonians at a fixed bare mass. It would be preferable to make the comparison at a fixed kinetic mass. However, Fig. 5 demonstrates that the $O(1/M)$, $O(1/M^2)$ and $O(1/M^3)$ Hamiltonians all give rise to the same relationship between the bare and kinetic masses, within the statistical uncertainties.

In Fig. 7, the spin splitting is plotted as a function of the bare heavy quark mass. The vacuum expectation value has not been removed from the c_{10} term. $O(1/M^2)$ and $O(1/M^3)$ terms provide small corrections to the spin splitting near $M=M_b$, but sizable ones near $M=M_c$, with an $O(1/M^3)$ contribution that is larger in magnitude than the $O(1/M^2)$ contribution.

According to Fig. 8, there are two $O(1/M^3)$ terms which dominate the large correction to the spin splitting: c_7 and c_{10}. The importance of c_{10} for the spin splitting is somewhat puzzling, since that term in the Hamiltonian is spin-independent. Some insight is gained by removing the vacuum expectation value from the c_{10} term [17], which is shown in Fig. 9 to remove almost the entire effect of the c_{10} term in the charm region. This small contribution of c_{10} to the spin splitting is to be expected for a spin-independent operator. Apparently the large effect of c_{10} in Fig. 8 is spurious, perhaps because the vacuum expectation value is not sufficiently small compared to the heavy quark mass.

To confirm this, recall Eq. (25) which describes the discretization of the heavy quark propagator. In the continuum limit, this propagation depends exponentially on the Hamiltonian. At a finite lattice spacing, Eq. (25) uses a linear approximation to the exponential of $a\,\delta H$. Following Ref. [3], the exponential of aH_0 was fit more precisely than a simple linear approximation, so that an instability could be avoided at small M. In Eq. (25), if the c_{10} term is subtracted from δH and added to H_0, then the spin splitting reproduces Fig. 9 rather than Fig. 8. [The values of the parameter n in Eq. (25) are not changed from what have been used throughout this work. For example, $n=3$ at $\beta=6.8$ and $n=4$ at $\beta=7.0$ in the charm region.] This supports the suspicion that the large

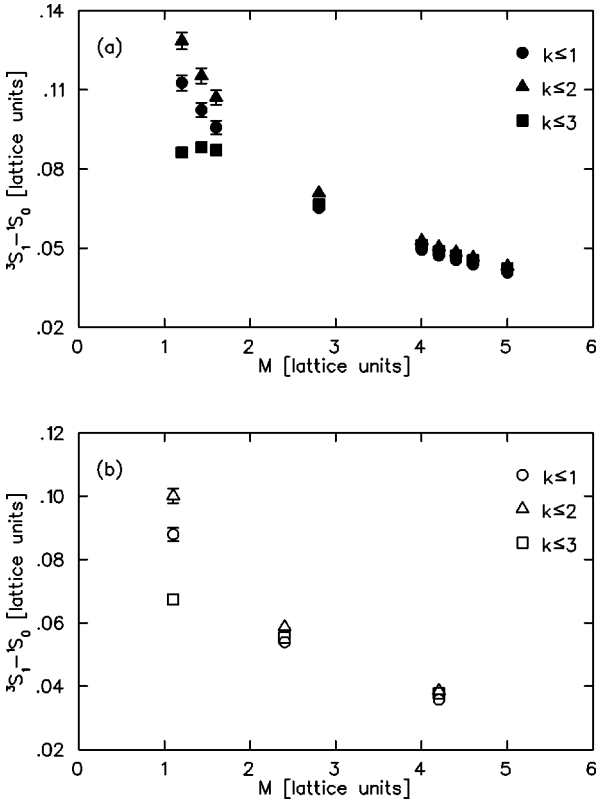

FIG. 7. The spin splitting of S-wave heavy-light mesons, from terms up to $O(1/M^k)$, with $k=1,2,3$. M is the bare heavy quark mass. Solid symbols denote data at $\beta=6.8$ and $\kappa=0.135$, while open symbols correspond to $\beta=7.0$ and $\kappa=0.134$. The vacuum expectation value has *not* been removed from the c_{10} term.

vacuum expectation value was causing a breakdown of the results in Fig. 8. The problem has thus been successfully overcome in two separate ways: by the explicit removal of the vacuum value from the Hamiltonian, or by a better-than-linear approximation to the exponential dependence of heavy quark propagation on the c_{10} term.

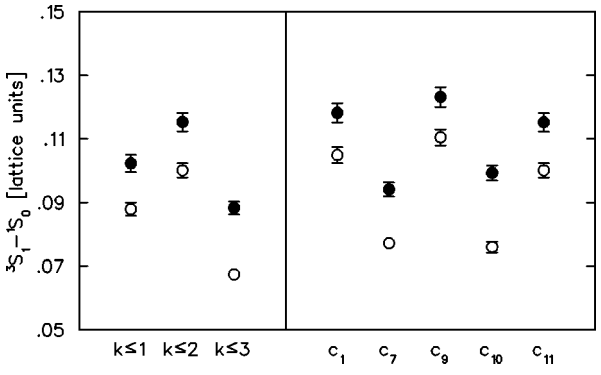

FIG. 8. The spin splitting of S-wave charmed mesons. Results are displayed from terms up to $O(1/M^k)$, with $k=1,2,3$. Solid symbols denote data at $\beta=6.8$, $\kappa=0.135$ and $aM=1.43$, while open symbols correspond to $\beta=7.0$, $\kappa=0.134$ and $aM=1.10$. To the right of the vertical line, the effect of adding each $O(1/M^3)$ term to the $O(1/M^2)$ Hamiltonian is shown individually. The vacuum expectation value has not been removed from the c_{10} term.

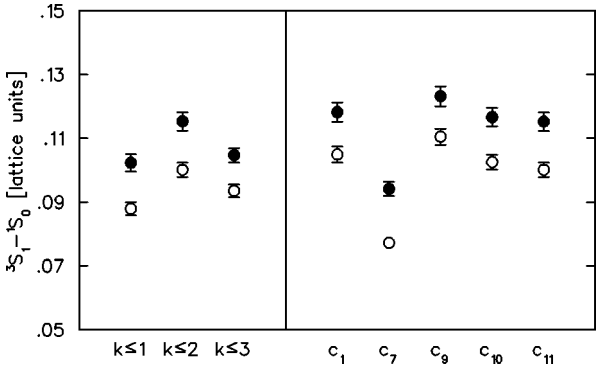

FIG. 9. These data are identical to Fig. 8 except that the vacuum expectation value has here been subtracted from the c_{10} term.

Figure 9 indicates that the spin splitting satisfies $|O(1/M^3)|<|O(1/M^2)|<|O(1/M)|$. This same ordering persists for all M values considered, as seen in Fig. 10. Notice in particular that the turnover of the $O(1/M^3)$ data near M_c is completely removed from Fig. 7 by correctly accounting for the vacuum value in the c_{10} term. Meanwhile, the data at $aM>2$ are not affected in a statistically-significant way. The $1/M$ expansion might now appear to be nicely convergent, but some caution is suggested due to the c_7 term, which is by itself larger in magnitude than the total $O(1/M^2)$ contribution to the spin splitting of a charmed meson.

It is interesting to consider the difference between squares

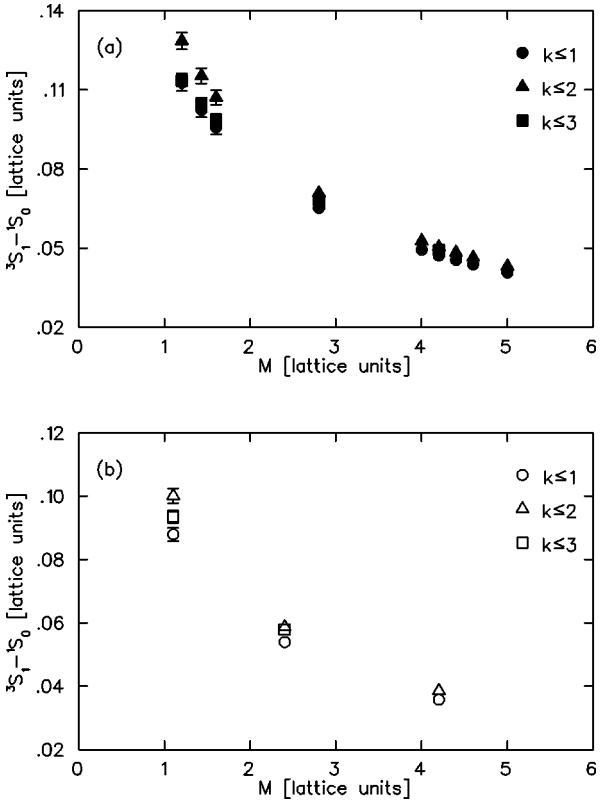

FIG. 10. These data are identical to Fig. 7 except that the vacuum expectation value has here been subtracted from the c_{10} term.

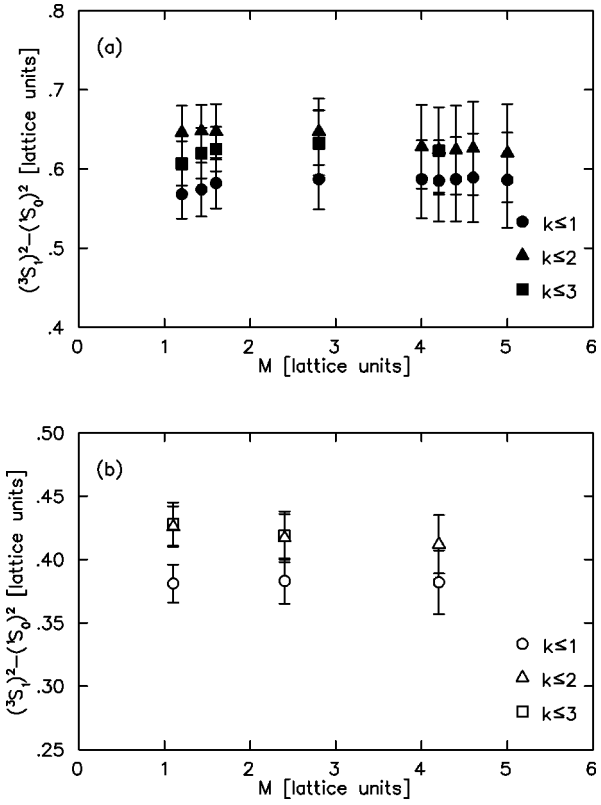

FIG. 11. The difference between squared masses of vector and pseudoscalar heavy-light mesons, from terms up to $O(1/M^k)$, with $k=1,2,3$. M is the bare heavy quark mass. Solid symbols denote data at $\beta=6.8$ and $\kappa=0.135$, while open symbols correspond to $\beta=7.0$ and $\kappa=0.134$. The vacuum expectation value has been subtracted from the c_{10} term.

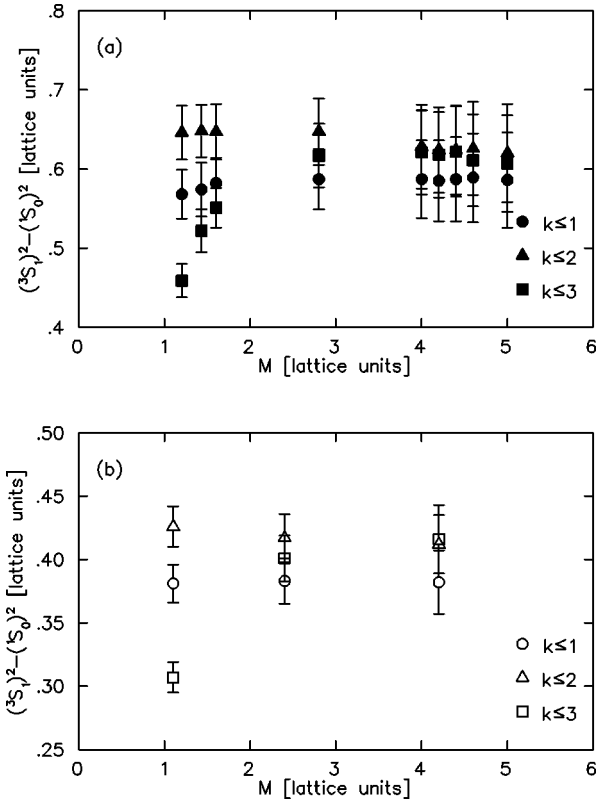

FIG. 12. These data are identical to Fig. 11 except that the vacuum expectation value has here *not* been subtracted from the c_{10} term.

of the $^3S_1$ and $^1S_0$ masses, which empirically is remarkably independent of the ''heavy'' quark mass:

$$(B^{+*})^2-(B^+)^2\approx(B^{0*})^2-(B^0)^2=0.48\ \text{GeV}^2 \quad (36)$$

$$(B_s^*)^2-(B_s)^2=0.51\ \text{GeV}^2 \quad (37)$$

$$(D^{+*})^2-(D^+)^2\approx(D^{0*})^2-(D^0)^2=0.55\ \text{GeV}^2 \quad (38)$$

$$(D_s^*)^2-(D_s)^2=0.59\ \text{GeV}^2 \quad (39)$$

$$(K^{+*})^2-(K^+)^2\approx(K^{0*})^2-(K^0)^2=0.56\ \text{GeV}^2 \quad (40)$$

$$(\rho^+)^2-(\pi^+)^2\approx(\rho^0)^2-(\pi^0)^2=0.57\ \text{GeV}^2. \quad (41)$$

In the extreme heavy quark limit, this result is easily understood using heavy quark symmetry: the spin splitting vanishes as $1/M$ while the meson masses themselves grow linearly with M, so the difference of squares is a constant,

$$m_V^2-m_P^2=(m_V-m_P)(m_V+m_P)=\text{const}+O(1/M). \quad (42)$$

For mesons containing only light quarks, the explanation is perhaps not so clear. Some authors have related it to chiral symmetry [18]. It should be noted that $m_V^2-m_P^2\approx$const is also a consequence of the nonrelativistic quark model with a linear potential (and no heavy quark assumptions).

The difference of squares arising from the present simulations is shown in Fig. 11 with the vacuum value subtracted from the c_{10} term, and for a particular light quark κ. [For all cases considered, the results are essentially independent of κ, in agreement with Eqs. (36)–(41).] The large errors are due to the required use of M_{kin} and they are correlated, as evidenced by the central values being constant to within a much smaller uncertainty than the quoted errors would require. In fact, the $O(1/M)$, $O(1/M^2)$ and $O(1/M^3)$ data are each constant for the full range of M values that were considered.

For the purpose of comparison, the same plot is displayed in Fig. 12, but without a proper treatment of the vacuum expectation value, i.e. with the vacuum value retained in the c_{10} term and the simple heavy quark propagation of Eq. (25). Erroneous results are clearly produced at $O(1/M^3)$ for $aM<2$.

For all of the observables under discussion in this work, the c_{11} term is essentially irrelevant, which may not be too surprising in light of its large numerical suppression factor in the Hamiltonian, Eq. (12).

Finally, to make the connection to experiment, it is necessary to interpolate to the strange quark mass (i.e., to κ_s),

TABLE III. Values for the physical masses and mass differences in MeV. The bare quark masses are set to $aM_c=1.43$, $aM_b=5.0$ at $\beta=6.8$, and $aM_c=1.10$, $aM_b=4.2$ at $\beta=7.0$. The Hamiltonian contains terms up to $O(1/M^k)$, where $k=1,2,3$. For charmed mesons, the vacuum value has been subtracted from the c_{10} term. The quoted errors include the uncertainties in κ_c, κ_s and a. (The uncertainties in κ_c and κ_s are negligible except for D_s-D and B_s-B.)

	D_s	D_s-D	D^*-D	$D_s^*-D_s$	B_s	B_s-B	B^*-B	$B_s^*-B_s$
				Experiment (Ref. [4])				
	1969	99,104	141,142	144	5369(2)	90(3)	46	47(4)
				$\beta=6.8$				
$k\leqslant 1$	2010(130)	96^{+6}_{-10}	92(6)	84(3)	5300(700)	75^{+9}_{-5}	37(4)	34(2)
$k\leqslant 2$	2000(110)	99^{+6}_{-13}	104(7)	95(4)	5300(700)	79^{+10}_{-9}	39(4)	36(2)
$k\leqslant 3$	2090(120)	98^{+6}_{-7}	100(6)	89(3)	5300(700)	79^{+8}_{-11}	39(4)	35(2)
				$\beta=7.0$, scaled by $a_{\rm hvy}$				
$k\leqslant 1$	1940(120)	111^{+7}_{-11}	100(10)	92(5)	5000(450)	86^{+8}_{-7}	40(4)	37(2)
$k\leqslant 2$	1920(110)	113^{+7}_{-11}	114(8)	105(5)	5000(450)	86^{+8}_{-7}	43(4)	40(2)
$k\leqslant 3$	2060(110)	113^{+8}_{-10}	111(7)	100(5)	5000(450)	86^{+8}_{-7}	42(4)	39(2)
				$\beta=7.0$, scaled by a_ρ				
$k\leqslant 1$	1760(100)	102^{+6}_{-11}	91(6)	84(4)	4500(400)	79^{+7}_{-6}	36(3)	34(2)
$k\leqslant 2$	1750(90)	103^{+6}_{-9}	104(6)	96(6)	4500(400)	79^{+7}_{-6}	39(4)	37(2)
$k\leqslant 3$	1880(90)	103^{+7}_{-8}	101(6)	91(4)	4500(400)	79^{+7}_{-6}	39(3)	36(2)

and to extrapolate to the limit of massless up and down quarks (κ_c). Interpolations are performed linearly between the two nearest κ values, and extrapolations are linear in all three available κ values. It is also necessary to determine the physical mass scale. For $\beta=6.8$, both the ρ meson mass and the charmonium $1P-1S$ mass splitting lead to the same physical scale ($a_\rho\approx a_{\rm hvy}$). Use of the bare heavy quark masses from quarkonium (Table II) gives the results of Table III.

At $\beta=6.8$, simulations up to $O(1/M)$, $O(1/M^2)$ and $O(1/M^3)$ each produce masses for both the D_s and B_s which are consistent with the experimental values, indicating that the bare charm and bottom masses from quarkonium physics are also relevant to heavy-light mesons. The light quark dependence at $\beta=6.8$, as probed by D_s-D and B_s-B, is also in reasonable agreement with experiment. The spin splittings are significantly smaller than experiment, which is a general feature of previous lattice results as well [5–9], and is often attributed to quenching.

The situation at $\beta=7.0$ is complicated by the fact that $a_\rho\neq a_{\rm hvy}$. In Table III, the lattice data are shown for both of these normalizations with the bare heavy quark masses fixed to the values obtained from quarkonium. The use of $a_{\rm hvy}$ produces D_s and B_s masses which agree nicely with experiment (as was found for $\beta=6.8$), whereas the data normalized to a_ρ clearly cannot produce accurate D_s and B_s masses when the bare masses are fixed by quarkonium.

Conversely, mass differences normalized to $a_{\rm hvy}$ tend to be larger than the results at $\beta=6.8$, whereas the a_ρ-normalized mass differences are found to scale remarkably well with respect to the $\beta=6.8$ results. This preference of the data for a_ρ is in accordance with the familiar notion that the dynamics of heavy-light mesons is governed by the light degrees of freedom, rather than by explicit heavy quark dynamics.

Perhaps the most satisfactory determination of mass differences at $\beta=7.0$ would be obtained by normalizing to a_ρ and retuning the bare mass to the heavy-light spectrum itself, with no reference to quarkonium. However, the possibly-problematic convergence of the $1/M$ expansion for charmed mesons precludes a more detailed effort in this direction at present. There is no retuning required at $\beta=6.8$, so at least in this case an unambiguous quantitative comparison to experiment can be made from the data in Table III, although concerns about the potentially-large $O(1/M^3)$ contributions (such as the c_7 term) must certainly be addressed.

In the work of Ishikawa *et al.* [6], a range of heavy quark masses were studied and it was found that the $O(1/M^2)$ terms increase the spin splitting relative to the $O(1/M)$ value, in agreement with what is reported here in Table III. The classically-complete set of $O(1/M^3)$ terms have now been included, and their total contribution is smaller in magnitude than $O(1/M^2)$. However, it has also been demonstrated that the small $O(1/M^3)$ contribution to the spin splitting results from a cancellation involving an individual term (the c_7 term) which is dangerously-larger in magnitude than $O(1/M^2)$.

V. CONCLUSIONS

The masses of $^1S_0$ and $^3S_1$ heavy-light mesons have been obtained from quenched lattice NRQCD at two lattice spacings, near 0.22 fm and 0.26 fm, using classically and tadpole-improved light quark and gauge field actions. Re-

sults were obtained separately at $O(1/M)$, $O(1/M^2)$ and $O(1/M^3)$. The effects of individual terms at $O(1/M^3)$ were also shown.

The simulations up to $O(1/M^2)$ support the existing knowledge of heavy-light S waves for lattice QCD. Masses are in qualitative agreement with experimental data, except that the spin splitting is noticeably smaller than experiment. This may be due, at least in part, to quenching.

The contributions of the $O(1/M^3)$ terms have not been studied in detail previously. A novel feature at this order is the existence of a large vacuum expectation value (in the c_{10} term) that shifts the heavy quark mass. Special care is needed when this vacuum value is present, particularly in the charm region. An important example is Fig. 8, where the vacuum value seems to make a sizable contribution to the S-wave spin splitting, but the effect was shown to be an artifact of the familiar discretization of $\exp(H\tau)$ in the heavy quark propagation.

It should be noted that the c_7 term also produces an $O(1/M^3)$ contribution to the spin splitting which is larger in magnitude than the total $O(1/M^2)$ piece. In fact, Fig. 8 indicates that this effect is very similar in size to the spurious contribution from the vacuum value in the c_{10} term, thus raising the question of whether the c_7 contribution might also contain some artifact related to the discretization of $\exp(H\tau)$. This systematic uncertainty has not been discussed in the literature to date, but might offer some important insight for the charmed spectrum calculation and also for charmonium.

Other possibilities for reducing the magnitude of the $O(1/M^3)$ corrections also deserve further study. In the present work, the coefficients of the NRQCD Hamiltonian have been approximated by their classical values, along with tadpole improvement. It would be interesting to see the effects of retaining one-loop perturbative or nonperturbative renormalization for these coefficients. One might also consider working at a smaller lattice spacing, although this will move the charm quark mass even further away from the heavy quark limit. (Recall that $aM_c=1.1$ at $\beta=7.0$. According to Ref. [11], $aM_c=0.81$ at $\beta=7.2$.) Some benefit might come from using a different definition of the tadpole factor, such as the Landau link definition, which increases aM_c at a fixed lattice spacing [11,19].

The existence of an individual $O(1/M^3)$ term whose contribution to the spin splitting is larger than the cumulative $O(1/M^2)$ effects, as was found in the present work, indicates that the application of lattice NRQCD to charmed mesons requires care.

ACKNOWLEDGMENTS

The authors are grateful to Howard Trottier for useful discussions and for access to his NRQCD codes, and to G. Peter Lepage for an important communication regarding the large vacuum expectation value at $O(1/M^3)$. This work was supported in part by the Natural Sciences and Engineering Research Council of Canada. R.L. also acknowledges support from the U.S. Department of Energy, contract DE-AC05-84ER40150.

[1] N. Isgur and M. B. Wise, Phys. Lett. B **232**, 113 (1989); **237**, 527 (1990).
[2] W. E. Caswell and G. P. Lepage, Phys. Lett. **167B**, 437 (1986); G. P. Lepage and B. A. Thacker, Nucl. Phys. B (Proc. Suppl.) **4**, 199 (1988); B. A. Thacker and G. P. Lepage, Phys. Rev. D **43**, 196 (1991); G. T. Bodwin, E. Braaten, and G. P. Lepage, *ibid.* **51**, 1125 (1995).
[3] G. P. Lepage, L. Magnea, C. Nakhleh, U. Magnea, and K. Hornbostel, Phys. Rev. D **46**, 4052 (1992).
[4] Particle Data Group, R. M. Barnett *et al.*, Phys. Rev. D **54**, 1 (1996).
[5] For a recent review, see A. Ali Khan, Nucl. Phys. B (Proc. Suppl.) **63**, 71 (1998).
[6] K.-I. Ishikawa, H. Matsufuru, T. Onogi, N. Yamada, and S. Hashimoto, Phys. Rev. D **56**, 7028 (1997).
[7] A. Ali Khan and T. Bhattacharya, Nucl. Phys. B (Proc. Suppl.) **53**, 368 (1997); J. Hein, *ibid.* **63**, 347 (1998).
[8] A. Ali Khan, C. T. H. Davies, S. Collins, J. Sloan, and J. Shigemitsu, Phys. Rev. D **53**, 6433 (1996).
[9] J. P. Ma and B. H. J. McKellar, Phys. Rev. D **57**, 6723 (1998).
[10] For a recent review, see C. T. H. Davies, Nucl. Phys. B (Proc. Suppl.) **60A**, 124 (1998).
[11] H. D. Trottier, Phys. Rev. D **55**, 6844 (1997).
[12] M. Lüscher and P. Weisz, Commun. Math. Phys. **97**, 59 (1985).
[13] G. P. Lepage and P. B. Mackenzie, Phys. Rev. D **48**, 2250 (1993).
[14] B. Sheikholeslami and R. Wohlert, Nucl. Phys. **B259**, 572 (1982).
[15] A. V. Manohar, Phys. Rev. D **56**, 230 (1997). See also C. Balzereit, Karlsruhe Report No. TTP98-02, hep-ph/9801436 (1998).
[16] C. T. H. Davies *et al.*, Phys. Rev. D **50**, 6963 (1994); **52**, 6519 (1995).
[17] We are grateful to G. P. Lepage for pointing this out to us, and for suggesting that it might have important implications for the spin splitting.
[18] D. C. Lewellen, Nucl. Phys. **B392**, 137 (1993); S. R. Beane, Duke University Report No. DUKE-TH-95-98, hep-ph/9512228.
[19] N. H. Shakespeare and H. D. Trottier, Simon Fraser University Report No. SFU HEP-151-98, hep-lat/9802038 (1998).